Energy 342 (2026) 139565

Contents lists available at ScienceDirect

Energy

journal homepage: www.elsevier.com/locate/energy

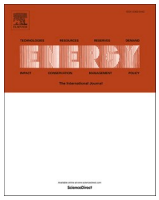

High-resolution atmospheric modelling reveals lower costs for renewable energy systems in Southern Africa

Shuying Chen [a,b,c,d,*], Klaus Goergen [a,c], Harrie-Jan Hendricks Franssen [a,c], David Franzmann [b,e], Christoph Winkler [b,e], Shitab Ishmam [b,e], Stefan Poll [a,c,f], Jochen Linssen [b], Harry Vereecken [a,c], Heidi Heinrichs [b,g]

[a] Institute of Bio- and Geosciences - Agrosphere (IBG-3), Forschungszentrum Jülich GmbH, 52425, Jülich, Germany
[b] Institute of Climate and Energy Systems - Jülich Systems Analysis (ICE-2), Forschungszentrum Jülich GmbH, 52425, Jülich, Germany
[c] Centre for High-Performance Scientific Computing in Terrestrial Systems, Geoverbund ABC/J, 52425, Jülich, Germany
[d] Department of Geosciences and Geography, RWTH Aachen University, 52056, Aachen, Germany
[e] Chair for Fuel Cells, Faculty of Mechanical Engineering, RWTH Aachen University, 52062, Aachen, Germany
[f] Jülich Supercomputing Centre (JSC) - Simulation and Data Laboratory Terrestrial Systems, Forschungszentrum Jülich GmbH, 52425, Jülich, Germany
[g] Chair for Energy Systems Analysis, Department of Mechanical Engineering, University of Siegen, 57076, Siegen, Germany

ARTICLE INFO

Keywords:
Wind energy
Solar energy
Energy systems design
Convection-permitting atmospheric modelling
ICON
ERA5

ABSTRACT

Expanding renewable energy in Africa is crucial for increasing electricity access and combating climate change, but scarce or coarse-resolution meteorological data often hinders accurate model-based renewable energy systems planning. Current assessments of the renewable energy potential and, subsequently, the design of renewable energy systems are typically based on coarse resolution reanalysis products such as ERA5 or MERRA-2. In this interdisciplinary study, we used the high-resolution validated meteorological data ICON-LAM from 2017 to 2019, based on physically consistent, atmospheric simulations with the ICON model, as an input to design cost-optimised renewable energy systems over southern Africa, and compare it to results obtained with ERA5 data. Higher wind energy potentials, averaging about 50 %, were found derived from ICON-LAM compared to ERA5, while solar energy potentials were similar. The cost-optimised energy system design using ICON-LAM inputs leads to a cost reduction of about 14 %, driven mainly by a 13 % lower battery capacity requirement, compared to using ERA5 – a result rooted in the cheaper wind energy revealed by ICON-LAM. This suggests that the cost of renewable energy systems may have been overestimated in the past, potentially hindering their efficient deployment. Hence, the study emphasises the importance of using high-resolution atmospheric modelling data sets as a decisive input for energy system planning.

1. Introduction

Africa remains the least electrified continent in the world [1]. Renewable energy presents a crucial opportunity to bridge this electricity supply gap, given the continent's vast and largely untapped renewable energy resources, as highlighted by recent participatory mapping [2] and multidisciplinary assessments [3] of green hydrogen cost-potentials from the H2Atlas project. The feasibility of distributed renewable energy systems further reinforces their potential to alleviate energy poverty in Africa by providing a cost-effective and technically viable alternative to centralised fossil-fuel-based power generation. Evidence from off-grid communities worldwide [4] and Africa [5] demonstrates their effectiveness in extending electricity access to previously un-electrified areas. Furthermore, the ongoing global transition toward carbon-neutral energy systems in response to climate change [6] underscores the urgency of a renewable energy-driven transformation in Africa. The expansion of renewable energy within African energy systems is therefore underpinned by multiple technical, economic, and policy-related factors.

Wind and solar are the most widely accessible renewable energy sources for electricity generation compared to others, such as biomass (biofuels and wastes), water (hydro and tidal), or geothermal heat [7]. However, both are variable renewable energy (VRE) resources, as they are highly dependent on weather conditions [8]. Energy systems in

* Corresponding author. Institute of Bio- and Geosciences - Agrosphere (IBG-3), Forschungszentrum Jülich GmbH, 52425, Jülich, Germany.
E-mail address: s.chen@fz-juelich.de (S. Chen).

https://doi.org/10.1016/j.energy.2025.139565
Received 14 May 2025; Received in revised form 13 November 2025; Accepted 4 December 2025
Available online 5 December 2025

general consist of interconnected networks of components involved in the production, conversion, delivery, and use of energy across various sectors, including power generation, heating/cooling, transportation, and industry [9]. Such energy systems are complex, as they consist of heterogeneous, spatio-temporally interconnected multi-scalar and multi-dimensional system components [10]. Incorporating power generated by VRE further complicates the energy systems design, implementation, and operation. Analysing complex energy systems with respect to VRE at a sufficient, decision-relevant level of detail is challenging.

How to deal with the internal fluctuation of power supply from VRE in an energy system has therefore been a long-standing and widespread discussion. Cochran et al. (2012) [11] identified best practices for integrating VRE into electricity markets, emphasising energy system flexibility, public engagement (especially for new transmission), and market design reforms. Sinsel et al. (2020) [12] reviewed the challenges and solution technologies for VRE integration, finding that the solution technologies vary significantly and interrelate, and that it is possible to identify groups of solution technologies for addressing challenge groups. More recently, Deguenon et al. (2023) [13] provided an overview of battery energy storage systems, including their characteristics, applications, and technologies suitable for grid-scale use. They found that lithium and flow batteries are the most widely used technologies, and that battery integration into the power grid could help achieve a VRE penetration rate of 40–50 %. Proposed viable solutions in the literature are, e.g., the self-complementarity of VRE, or the inclusion of backup systems, such as a storage system using battery or “power-to-x” [14], as well as dispatchable power systems like fossil-fired power plants [15] and hydropower plants [16]. To build reliable energy systems, the key lies in successfully identifying the self-complementarity of VRE sources, specifically, how their total power generation varies within the energy systems.

In this context, previous research has explored the geophysical constraints of the reliability of solar and wind energy in terms of their hybridisation, i.e. how both sources may complement each other, at both global [17] and regional scales [18]. The complementarity of wind and solar energy has been, for example, analysed for historical periods based on MERRA-2 reanalysis [19] and dynamical downscaling simulations with regional climate models [20]. For the investigation of future periods of wind and solar energy complementarity, simulations from the sixth phase of the Coupled Model Intercomparison Project (CMIP6) have been used by Costoya et al. [21]. The complementarity of VRE resulting in extremely low generation is also of interest, for example, Richardson et al. [22] identified solar and wind energy “droughts” under the influence of different weather conditions and climate modes for Australia. For a comprehensive review of the complementarity analysis of VRE, readers are referred to Jurasz et al. [23], where different types of complementarity – temporal, spatial, and spatiotemporal – between renewable energy sources are introduced, along with metrics for assessing complementarity. In this study, the self-complementarity of VRE is defined as the hybridisation of solar and wind power generation within a given region, emphasising its role in optimising energy balance at a local scale.

Many studies on VRE complementarity analysis originate from the geoscience or meteorology realm and have not incorporated recent advances from the field of renewable energy assessment. For example, analyses in these studies are based solely on the gridded meteorological data, rather than considering the land eligibility [24] and siting of VRE plants [25] as well, and usually the involved energy systems are considered in an idealised approach without considering real costs. However, these factors are highly relevant for the design of a real-world energy system. In contrast, previous studies dealing with VRE complementarity within the energy realm might incorporate the latest findings from renewable energy assessments, but they often rely directly on the available meteorological data sets for their regions of interest, usually coarse-resolution global reanalysis products [26]. This is the 1st research gap we identified. The present study addresses it by combining recent developments from both fields. Specifically, it integrates existing results on VRE land eligibility and plant location identification from Winkler et al. [2] with cost-optimised energy system modelling for VRE complementarity analysis, driven by a dedicated kilometre-scale high--resolution physically consistent meteorological data set.

To build an affordable, reliable, and sustainable energy system in Africa, in accordance with goal seven of the United Nations Sustainable Development Goals (SDGs), the spatial and temporal variability of VRE potential and the self-complementarity of VRE feed-in power time series need to be accurately resolved to optimise the energy system design. This energy system optimisation implies the necessity of accurate meteorological data from which reliable VRE information can be derived. Additionally, advances in microgrids and energy management systems that optimise control strategies for energy systems using metaheuristics, fuzzy logic, or bio-inspired algorithms greatly improve system performance in terms of cost, reliability, and renewable integration (e.g., Fuzzy logic-based energy management [27] or optimal battery management using the Modified Slime Mould Algorithm [28]). These works also rely heavily on accurate VRE generation profiles. However, existing meteorological data sets over Africa used to estimate VRE generation are often characterised by coarse spatial resolution [29] and data gaps [25].

The limited availability of reliable, high-resolution meteorological data significantly constrains the accuracy of energy system modelling for energy system design and management in Africa. The impact of using better-resolved data products on energy system modelling remains unknown, representing the 2nd research gap identified in this study. To address this 2nd research gap, the present work examines how different meteorological data products at varying spatial resolutions influence energy systems design. The state-of-the-art global reanalysis ERA5 (referred to as ERA5_ori) [30], its statistical downscaling variants ERA5_GWA (using the Global Wind Atlas [31]) and ERA5_GSA (using the Global Solar Atlas [32]), collectively referred to as ERA5_adpt, and a dedicated high-resolution dynamically downscaled product based on ICON simulations in limited area mode (ICON-LAM) [33] are examined.

A previous study already indicated higher onshore wind energy potentials using high-resolution meteorological data from ICON-LAM simulations compared to ERA5_ori and ERA5_GWA [34]. Based on these results, this study hypothesises that the higher wind energy potential revealed by ICON-LAM would substantially influence the cost-optimised design of the local energy system compared with other widely used, coarse-resolution data sets. Southern Africa is chosen as the focus area due to the availability of the high-resolution ICON-LAM simulations. The region may serve as a pilot area for the entire African continent.

The level of detail that model-based energy systems planning can incorporate is not only dependent on the quality of the VRE information, which is constrained by meteorological data sets, but also on computational capacity, computational methods for optimisation, and energy system-related data availability [35]. In large-scale energy systems models, typically at the national level, it is usual to use clustered or aggregated spatial data due to the high computational cost [35]. The spatial granularity of energy systems, often referred to as energy system nodes, is predefined, with calculations performed at the level of these nodes. The internal structure of the components within these nodes is typically disregarded. Likewise, this study defines administrative provinces as the energy system nodes and the energy system modelling is performed for each such province in southern Africa.

This study begins with an analysis comparing the wind and solar potential maps derived from ICON-LAM and ERA5 data (section 3.1). The motivation is to illustrate the maximum possible amount of VRE potential in southern Africa. Then, the complementarity analysis of solar and wind energy over southern Africa is carried out by incorporating the representative future electricity demand time series projected for the year 2050 for southern Africa. A cost-optimised renewable energy

system is designed for each province in southern Africa, with power generation from VRE and power storage from batteries considered to meet the projected regional electricity demand. The underlying VRE complementarity designed in this cost-optimised energy system is able to address both a reliable electricity supply and minimum overall costs. To evaluate the direct impact on local energy systems, this study holds assumptions that power transmission from generation to consumers is lossless within a region and that there is no power exchange between regions, following the works in Ishmam et al. [3] and Winkler et al. [2]. The cost and design of the energy system are compared based on the wind and solar VRE from different meteorological data sets (section 3.2 and 3.3). Finally, the daily time series of the renewable energy systems in terms of meeting the electricity demand shares of wind energy, solar energy, and battery (dis)charge are further investigated and compared (section 3.4).

2. Materials and methods

Three meteorological data sets are used in this study. These data differ in terms of their production methodology, as indicated by their data type: reanalysis product ERA5, statistical downscaling products ERA5_GWA and ERA5_GSA, and dynamical downscaling product ICON-LAM. The varying spatial resolutions and levels of detail in these products also make the comparison of the derived results particularly noteworthy.

2.1. Meteorological data sets

ERA5 [30] is a state-of-the-art global reanalysis product (ERA5_ori). With a temporal resolution of 1 h and a spatial resolution of 31 km, it has been widely used in Renewable Energy Potential (REP) assessments, e.g., Ref. [36]. The new ERA6 reanalysis is expected to replace ERA5 in 2027, with grid space reduced to half (close to 15 km) that of ERA5 [37]. The Global Wind Atlas [31] and Global Solar Atlas [32], both with a nominal spatial resolution of 250 m and long-term mean temporal averages are also frequently used information for REP analysis, for instance Ref. [38]. These global atlases (Wind: GWA, Solar: GSA) are integrated with a statistical downscaling approach [39] to overcome the coarse spatial resolution in ERA5. Following this approach, the long-term mean ratios of the global atlases to ERA5_ori, i.e., GWA/ERA5_ori and GSA/ERA5_ori, are first calculated and then multiplied with the ERA5_ori time series to obtain ERA5_GWA and ERA5_GSA (collectively referred to as ERA5_adpt).

High-resolution, i.e., convection-permitting or, interchangeably, kilometre-scale, meteorological data are scarce for Africa. Pan-African simulations are, e.g., by Stratton et al. [40] and Kendon et al. [41] at 4.5 km resolution. For this study, a dedicated high-resolution dynamical downscaling atmospheric simulation experiment over southern Africa was performed by Chen et al. [33] using the ICON model [42] in Limited Area Mode (ICON-LAM) at a convection-permitting resolution of 3.3 km. The ICON-LAM simulation is driven by the global initialised analysis from the German Weather Service (DWD) and uses a numerical weather prediction configuration of DWD. Chen et al. [33] give a detailed overview of the experiment setup and configuration, including an extensive evaluation of near-surface wind and solar irradiance, which demonstrates the suitability of the ICON-LAM 2017 to 2019 data for REP analysis. In Chen et al. [34], further evaluations show that ICON-LAM more accurately reproduces observed wind speed closer to the wind turbine height, as well as the derived wind power, when using a state-of-the-art renewable energy simulation model, compared to commonly used data sets.

The model domain of the ICON-LAM simulations defines the spatial focus of this study. It encompasses southern Africa below about 16° south, i.e., countries Namibia, Botswana, South Africa, Lesotho, and Eswatini are fully covered, and Zimbabwe and Mozambique are partially covered, and hence included in the study with a total of 65 provinces. This is referred to as southern Africa. The location and details of these countries and their provinces are shown in Fig. S1 and Table S1. Additionally, the results presentation does not include the 14 outermost grid cells of the model domain that serve as the lateral boundary conditions relaxation zone. The details of the model domain setup were documented in Ref. [33].

The time span of the ICON-LAM simulations - from 2017 to 2019 - defines the temporal focus of this study. The selection of the period for conducting ICON-LAM simulations was based on the availability of the forcing data of the ICON-LAM simulation and the representation of meteorological conditions with respect to wind and solar energy generation in the recent 30 years, in order to ensure a robust energy system analysis. As detailed by Chen et al. [33] the year 2019 was identified as generally above the 30-year average, 2017 below, and 2018 close to average, based on total surface global solar irradiance from ERA5. In comparison, wind speed at 100 m also showed a clear difference between these 3 years, although with more spatial heterogeneity.

2.2. The wind and solar power calculation and the REP estimation

The renewable energy simulation model RESKit [43] is employed to calculate wind and solar power in this study. In the RESKit model wind workflow (originally built by Ref. [39], updated by Ref. [44]), the 100 m wind speed is logarithmically scaled to the wind turbine hub height, and the wind power generated by the wind turbine is then derived according to a synthetic power curve – wind power as a function of wind speed. In the RESKit solar workflow [45], the solar irradiance received on top of the solar photovoltaic (PV) panels is first determined, and then the solar power generated by the solar PV panels is calculated accordingly using the law of photoelectric conversion. Other system-level loss factors are also considered, such as drops in PV panel photoelectric conversion efficiency due to the unfavourable ambient air temperature, losses from the inverter when converting direct current (DC) to alternating current (AC), and losses from soiling on the solar PV panels.

Based on the land eligibility and placement identification analyses performed by Winkler et al. [2], we calculate in total of 1,829,467 wind turbines and 748,388 km^2 solar PV panels in southern Africa that are eligible for the installation of the onshore wind and open-field solar PV energy placements. Advanced wind turbines and solar PV panel modules, which are available from the laboratory or manufacturer and are barely installed now but may be widely used in the future, are selected to be simulated with the RESKit model. Table 1 details key parameters of advanced wind turbine and PV panel technologies that are used in this study. The baseline wind turbine has turbine parameters predicted for 2035 (as proposed by Ref. [46] and used in Ref. [34]). The solar PV module features solar power conversion efficiency projected for 2050 [45]. Utilising all the eligible placements for the installation of wind and solar farms with advanced wind and solar energy technologies, the onshore wind and open-field solar PV energy potentials are estimated using the RESKit model over southern Africa with the ERA5_ori,

Table 1
Key parameters of anticipated advanced wind turbine and PV panel technologies. Note that all simulated wind turbines have deviating parameters from the baseline configuration that lead to a local maximum wind resource harvesting efficiency.

Design	Value
Baseline wind turbine:	
Hub Height	130 m
Rotor Diameter	174 m
Capacity	5500 kW
Specific Power	231.3 W m^{-2}
Solar PV panel design:	
Solar PV module	WINAICO WSx-240P6 [45]
Conversion rate	Projected for 2050
Capacity	Proportional to the available land area at 20 m^2/kWpeak

ERA5_adpt, and ICON-LAM datasets.

2.3. Spatially resolved electricity demand and time series for 2050

A basis for any energy system optimisation is electricity demand data. The annual sub-national disaggregated electricity demand data for the study region of southern Africa is sourced from Ishmam [47]. The annual electricity demand projections are built upon the Net Zero 2050 scenario provided by the Network for Greening the Financial System (NGFS) Scenario Framework (data source [48] and technical documentation [49]). These projections consider electricity demand from residential, commercial, agricultural, manufacturing, service, and transportation sectors. Geospatial proxies such as level of access to electricity, population density, CO2 emissions distribution, gross domestic product (GDP) distribution, etc., corresponding to these sectors, are then utilised to disaggregate the annual national electricity demand to the administrative level 1 (GID-1), i.e., provinces.

Hourly load curve data were then obtained from Toktarova et al. [50] for each country and adjusted to the UTC time zone to match the time zone of the generation time series. It is important to note that the shapes of these load curves may change over time as access to electricity improves and as the industrial and service sectors of countries grow, along with advancements in energy efficiency. However, for the purposes of this study, the load profiles have been retained in their current form and then scaled to align with the projected annual disaggregated demand in 2050. For in-depth information regarding the demand disaggregation methodology, please refer to Ishmam [47].

To illustrate the electricity demand, the spatially resolved hourly electricity demand time series for 2050 have been summed up over the entire southern Africa study domain as well as over individual countries in the study region (Fig. 1). All time series utilised in this study are in UTC. The annual cycle for the whole region shows the highest values during the austral winter (Fig. 1a). The country of South Africa is projected to exhibit the highest electricity demand in southern Africa by 2050, estimated at 342 TWh year^{-1}, about 86 % of the total annual electricity demand in the region. Due to scale, for better visibility, the electricity demand time series of the remaining study area countries are also shown in Fig. 1b, with the highest values during the austral spring and summer when cooling demand is highest.

Hourly fluctuations in electricity demand for all of southern Africa, South Africa, and the Western Cape province, which is the economic hub of South Africa, are shown in Fig. 2. The hourly electricity demand displays a discernible diurnal cycle, with a reduced nighttime demand from approximately 02:00 to 07:00. Expectedly, there is a contrast in energy demand between weekdays and weekends; also, public holidays stand out. A slight seasonal cycle is visible with an increased electricity demand during the austral winter months and evenings.

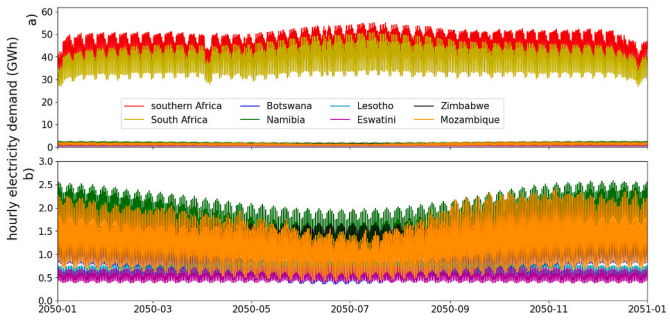

Fig. 1. a) Projected total hourly electricity demand for 2050 for the entire southern Africa and those countries that are fully or partly covered by the ICON-LAM model domain, b) Same as in a) but zoomed in for countries with relatively lower electricity demand [47].

2.4. Energy systems modelling

The power time series calculated by the RESKit model for onshore wind energy and open-field solar PV energy serve as the basis for designing optimal energy systems. This study focuses on a future 2050 electricity demand scenario as introduced in the previous section. To alleviate the computational burden in the energy system modelling, power time series of wind and solar energy are clustered over each energy system node (province). Following studies of Ryberg [45] and Franzmann et al. [51], segmented average clustering is used in this study: For each of the energy system nodes, the annual Full Load Hours (FLH) of every individual wind and solar placement within an analysis region is calculated and ordered from the highest to the lowest. They are further serially divided into N groups with similar FLH members. The power time series belonging to the same FLH group are averaged as the group representative. The class number used as N is set to 10 and 3 for wind and solar power time series clustering, respectively.

After getting the representative wind and solar power time series in each energy system node, the energy system framework, ETHOS.FINE (code repository [52] and documentation [53]) and the solver Gurobi [54] are used to derive cost-optimised energy systems based on wind energy, solar energy, and battery storage for each province independently in the year 2050. ETHOS.FINE minimises the total annual costs while fulfilling the aforementioned provincial electricity demand based on the restricted maximum operation time series of renewable energy generation and on the ability to use curtailment. Due to the one-node spatial resolution of the energy systems, power transmission losses from power plants to power consumers and power transmission between provinces are not considered to solely focusing on the impact of different weather data products. The techno-economic parameters for calculating the total annual costs follow published works in Refs. [55,56].

3. Results and discussion

In this study, the impact of three different meteorological data sets on the design of a renewable energy system over southern Africa is investigated. For this, an energy system considering wind energy, solar energy, and battery storage is designed in a cost-optimised way to meet 100 % of the provincial 2050 electricity demand scenario in the 65 provinces of southern Africa. Three meteorological data sets for 2017 to 2019 are used to calculate the solar and wind power generation, serving as input for the design of the cost-optimised energy system.

The analyses for this study begin with an investigation of the maximum possible wind and solar energy potential in the study domain. Then, the complementarity of wind and solar energy with respect to meeting local electricity demand at the lowest system cost is analysed. The cost of the system, the required capacity of the wind, solar, and battery components, and the share of electricity generation/(dis)charge over time are compared and discussed.

3.1. ICON-LAM reveals higher onshore wind and similar open-field solar PV energy potential

Considerable differences are found between the maximum harvestable wind energy potentials estimated from the three data sets, as shown in Fig. 3 (the corresponding percentage difference can be found in Fig. S2). These results are consistent with the findings of Chen et al. [34]. In contrast, similar maximum harvestable solar energy potentials are shown in Fig. 3 (also in Fig. S2), estimated from different data sets. They are actually almost identical, with few detectable differences, and very similar spatial distributions of solar irradiance for the data sets were also shown in Chen et al. [33]. Comparable results for wind and solar energy potential, as indicated by the capacity factor [57] – the ratio of actual power generated to the nominal generation capacity – is shown in Fig. S3. The solar and wind energy potential maps in Fig. 3, S2, and S3 are produced based on a total of 1.8 million eligible wind turbine

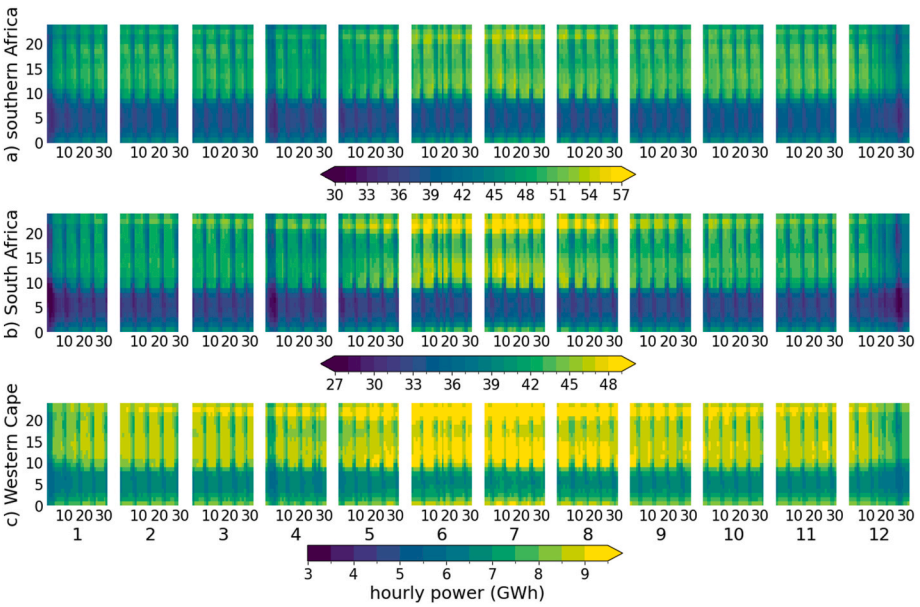

Fig. 2. Hourly electricity demand time series for a) southern Africa, b) South Africa, and c) Western Cape as projected for 2050, with days of the year aggregated by month shown on the x-axis and hours of the day shown on the y-axis. Please note the different scales of the colour bars used in the figure.

placements and 0.74 million km^2 solar photovoltaic (PV) panel placements in southern Africa, respectively; values for each of these eligible placements are plotted, resulting in eventually a continuous map made up of many individual data points.

When comparing wind energy potentials derived from the three data sets, the coarse spatial resolution of ERA5_ori (31 km) becomes obvious, as details of wind energy potentials are hardly visible compared to the other two high spatial resolution data sets. However, the general patterns of contrasting high and low wind energy potentials are consistent between the data sets. In addition, ICON-LAM shows generally a higher wind energy potential over the entire study domain, while ERA5_GWA partially agrees with ICON-LAM. The respective spatial mean annual wind energy potential derived from ERA5_ori, ERA5_GWA, and ICON-LAM are 12.39 GWh/turbine, 11.37 GWh/turbine, and 17.02 GWh/turbine, with all 1.8 million eligible wind turbine placements considered.

Relatively large solar energy potentials within our study area exist in western South Africa and small parts of southern Namibia and Botswana (Fig. 3b, d, and 3f). Locations along the south coast, eastern South Africa, Zimbabwe, and southern Mozambique are less favourable for solar energy installations. These locations correspond to the general atmospheric circulation patterns and the spatial patterns of precipitation in southern Africa (Fig. S1 in Chen et al. [33]), where clouds reduce the incoming solar radiation. The agreement in the spatial patterns of solar energy potentials derived from three data sets indicates that large-scale anticyclonic circulation patterns with high-pressure clear-sky conditions in the southwest of the domain are well represented by ERA5 and ICON-LAM.

3.2. Lower annual costs in energy systems derived from ICON-LAM

The total annual costs and the individual shares of different technologies (wind, solar, battery) of these cost-optimised energy systems in southern Africa, derived from different meteorological data sets, are shown in Fig. 4. A scaled axis is additionally provided in Fig. 4, since values of provinces from South Africa, due to its dominant electricity demand in all of southern Africa (see Fig. 1), exceed the other countries as outliers. Out of the 65 provinces of our southern African study domain, 52 are considered capable of supporting a cost-optimised energy system that meets 100 % of the regional 2050 scenario electricity demand by exploiting only renewable energy sources, i.e., the local wind and solar energy potentials per region, combined with battery installations. Table S1 details the basic information for each province and indicates whether the cost-optimised energy system would be feasible to build or not. If the cost-optimised energy system cannot be built, the reasons are also documented, which are usually rooted in no eligible wind and solar placements at all or the optimisation being proven infeasible or unbounded.

In general, cost-optimised energy systems designed based on the ICON-LAM data set have lower total annual costs compared to the other two data sets. The annual cost from ICON-LAM is 11 % Euros/a less than from ERA5_adpt and 16 % Euros/a less than from ERA5_ori, averaged over three years for all provinces. Cost-optimised energy systems derived from ICON-LAM have more wind energy capacity (comparable to ERA5_adpt and 9 % more than ERA5_ori) and less solar energy capacity (13 % less than ERA5_adpt and 23 % less than ERA5_ori) compared to the two ERA5 variants. In addition, the required battery capacity of cost-optimised energy systems derived from ICON-LAM is less than the other two (9 % less than ERA5_adpt and 17 % less than ERA5_ori).

To investigate the reasons behind the lower annual costs of energy systems designed with ICON-LAM, a comprehensive analysis of annual operational characteristics of energy systems derived from different meteorological data sets is presented in Fig. 5. The figure shows the full load hours (FLHs), levelized cost of electricity (LCOE), VRE potential utilisation rate, and curtailment rate for wind and solar technologies, and (dis)charge frequency and levelized cost of storage for battery technology, used in the energy systems. More FLHs of wind energy (Fig. 5a), pointing to cheaper wind energy (Fig. 5d), are available for use in the cost-optimised energy systems designed with ICON-LAM (on average, 1.3 times greater than the others), which is consistent with the findings of Chen et al. [34] that high-resolution kilometre-scale atmospheric modelling over southern Africa yields higher wind energy potentials. Meanwhile, lower required battery capacity (Fig. 4), about 200 MW on average, indicates that wind and solar power estimated from ICON-LAM better complement each other in meeting demand, as less backup (battery) capacity is needed, leading to lower system cost. This is further confirmed by the lowest average battery (dis)charge frequency (Fig. 5c) of energy systems designed with ICON-LAM, as compared to with other ERA5 variants.

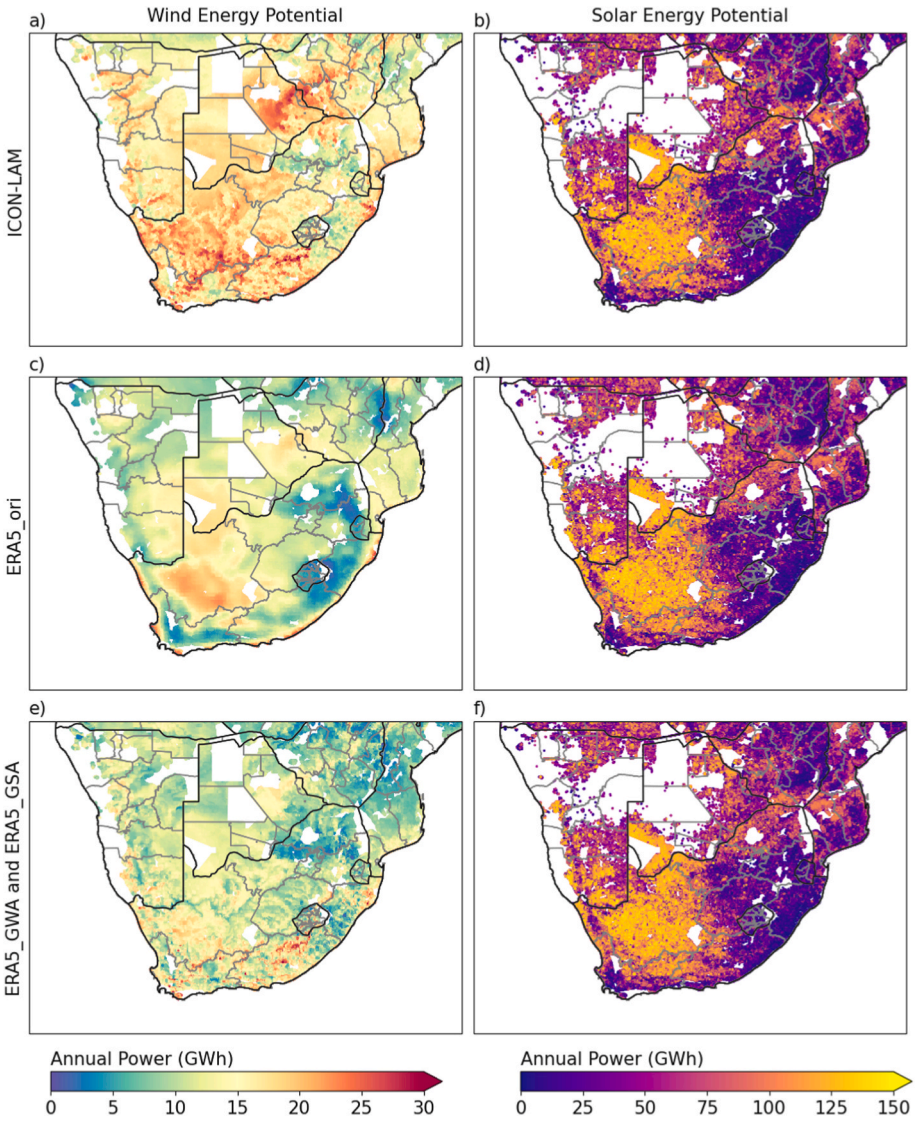

Fig. 3. Comparison of estimated 2017–2019 average annual total power derived from ERA5_ori, ERA5_GWA/_GSA, and ICON-LAM simulated by the RESKit model wind and solar workflows across all eligible wind turbine and solar PV panel placements in southern Africa. Black lines are country borders, and grey lines are provinces in southern Africa used as energy system nodes in the study. Names of the countries and provinces included in this study are shown in Fig. S1 and Table S1. All maps are made up of multiple colour-coded site-specific information, where each data point represents one wind turbine (a total of 1.8 million turbines) in Fig. 3a, c, and 3e and one area of solar PV panels (a total of 0.74 million km^2 panels) in Fig. 3b, d, and 3f, visually appearing as continuous data fields.

Generally, all three data sets agree with each other that a low potential utilisation rate with a maximum around 7 % from the total wind and solar potentials (Fig. 5g and h), combined with an appropriate amount of installed battery capacity, is sufficient to meet the electricity demand for all provinces in southern Africa. Furthermore, on average more than half of the solar energy is curtailed (Fig. 5k), while a relatively higher proportion of wind energy (curtailment rate $<$35 % in most provinces) is utilised (Fig. 5j), due to the nature of their generation, where solar energy is almost only available during the day while wind energy does not have a relatively strong periodic signal. Little interannual variation is observed regarding the cost and design (Fig. 4) and the operational characteristics (Fig. 5) of cost-optimised energy systems based on data from 2017 to 2019.

3.3. *Spatially varied costs and design of energy systems using different meteorological inputs*

Fig. 6 presents the cost-optimised energy system for each southern African province in 2017, derived from three meteorological data sets. Results for 2018 and 2019 are shown in Figs. S4 and S5, which display in essence the same patterns. South African provinces, especially Western Cape and KwaZulu-Natal, have the highest total annual costs compared to other provinces in southern Africa, but ICON-LAM lowers the average costs by 11 % and 16 % compared to ERA5_adpt and ERA5_ori, respectively. The cost differences between energy systems derived from two ERA5 variants are relatively small, around 5 %. Given the significantly lower electricity demand compared to South African provinces, other provinces in southern Africa beyond South Africa show insignificant variations in terms of energy system design and costs. The following analysis, therefore, focuses on South Africa.

According to ICON-LAM (Fig. 6b), the southern coastal provinces of South Africa (Western Cape, Eastern Cape, and KwaZulu-Natal) exhibit greater wind energy capacity installations than those based on both ERA5 (Fig. 6f and j), with maximum differences of 48 % and minimum of 8 %. Meanwhile, the northern four provinces of South Africa demonstrate slightly lower wind energy capacity installation from ICON-LAM compared to ERA5_adpt (on average, 17 %) and to ERA5_ori (on average, 8 %). In contrast, the energy systems derived from ICON-LAM

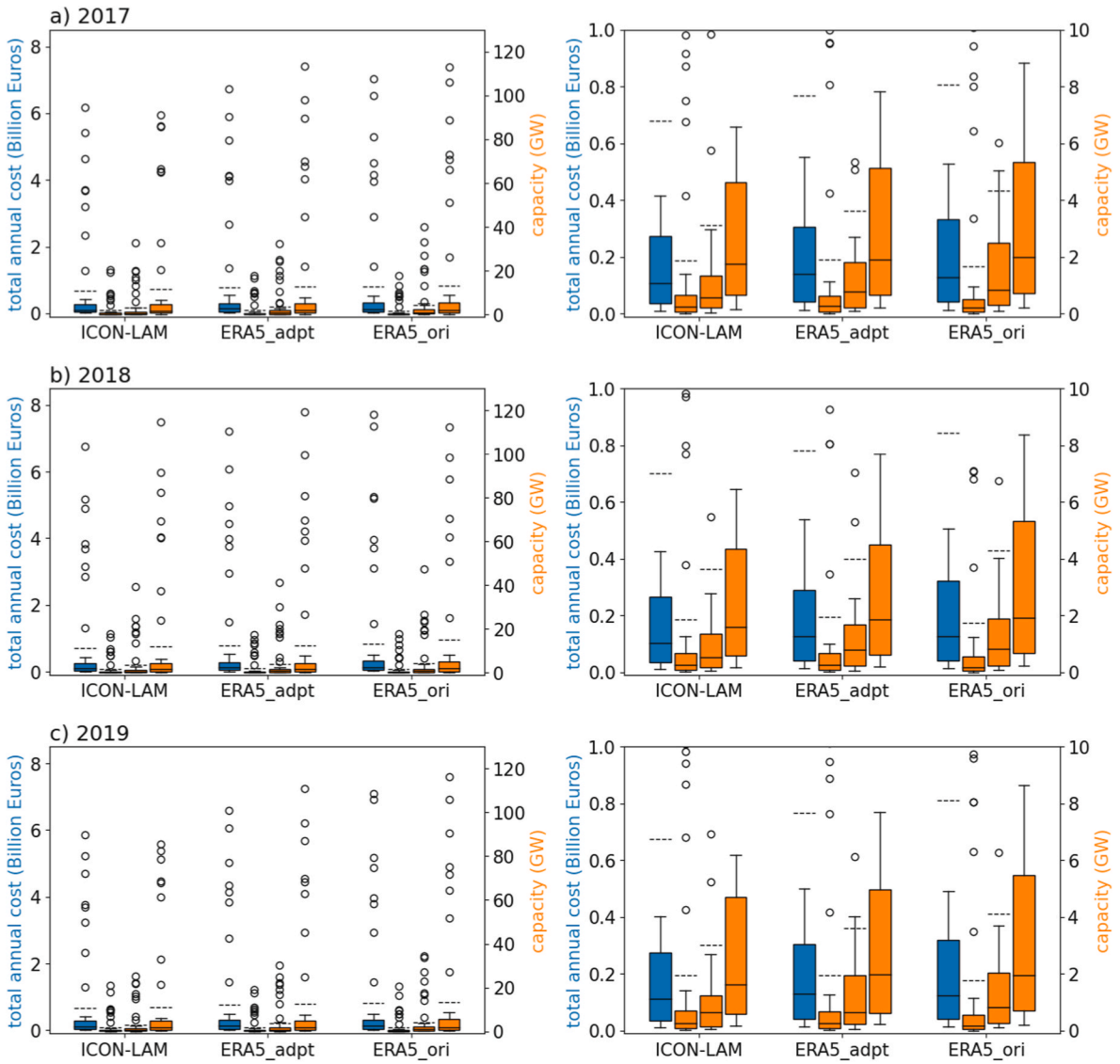

Fig. 4. The energy system's total annual cost (Billion Euros) (blue bar) and the installed capacity (GW) of wind energy, solar energy, and battery (respective orange bars from left to right) for the cost-optimised regional energy system derived from different meteorological products for the three weather reference years a) 2017, b) 2018, and c) 2019. The first column contains all data points, while the second column zooms in on a range from 0 to 1 billion Euros and 0 to 10 GW capacity for a better presentation of the data. Each box extends from the first quartile (25th percentile) to the third quartile (75th percentile) of the data, with the median shown as a solid line inside. The whiskers are set at 1.5 times the interquartile range (IQR, the difference between the 75th and 25th percentiles) above the 75th percentile and below the 25th percentile, i.e., a box ends at ± 1.5*IQR. Data points are marked as outliers if they exceed the range defined by two whiskers. Dashed lines are the averages of all underlying data points for the corresponding box plots.

(Fig. 6c) require less solar energy capacity compared to ERA5_adpt (Fig. 6g) and especially ERA5_ori (Fig. 6k) of 9 % and 24 % on average, respectively. A similar behaviour is observed for the required battery capacities, with a slight increase only in the northernmost province (Limpopo, 6 %) using ICON-LAM (Fig. 6d) compared to ERA5_adpt (Fig. 6h). This is mainly due to the cheaper wind energy as well as better complemented wind and solar energy that ICON-LAM delivers compared with ERA5 variants, as indicated in section 3.2 based on Figs. 4 and 5.

3.4. ICON-LAM: increased wind and reduced solar energy contribution for meeting demand over time

To illustrate how hourly electricity demand is met using a combination of technologies and how the energy system is cost-optimised through the curtailment of VRE power generation, a random subset of time series data is selected from the cost-optimised energy system in the Western Cape province of South Africa. Fig. 7 shows energy systems cost-optimised by energy system modelling based on VRE potentials derived from ICON-LAM, ERA5_adpt, and ERA5_ori. The total power available in the system is the combined generation from wind energy and solar energy, as well as the charging (negative) or discharging (positive) from the battery. The electricity demand is depicted in an inverse manner, representing demand as an energy sink. Since the electricity demand is met 100 % on an hourly basis, as illustrated in Fig. 7, the lines representing the total power available in the system and the electricity demand are two symmetric lines with respect to the zero line. The energy system limits the amount of wind and solar power it generates to balance costs and operational efficiency. The maximum possible wind and solar power are higher than the actual power generated, and the difference is curtailment. This curtailment helps the system to minimise costs.

After illustrating the sample time series in the cost-optimised energy systems, how different energy systems optimised with different

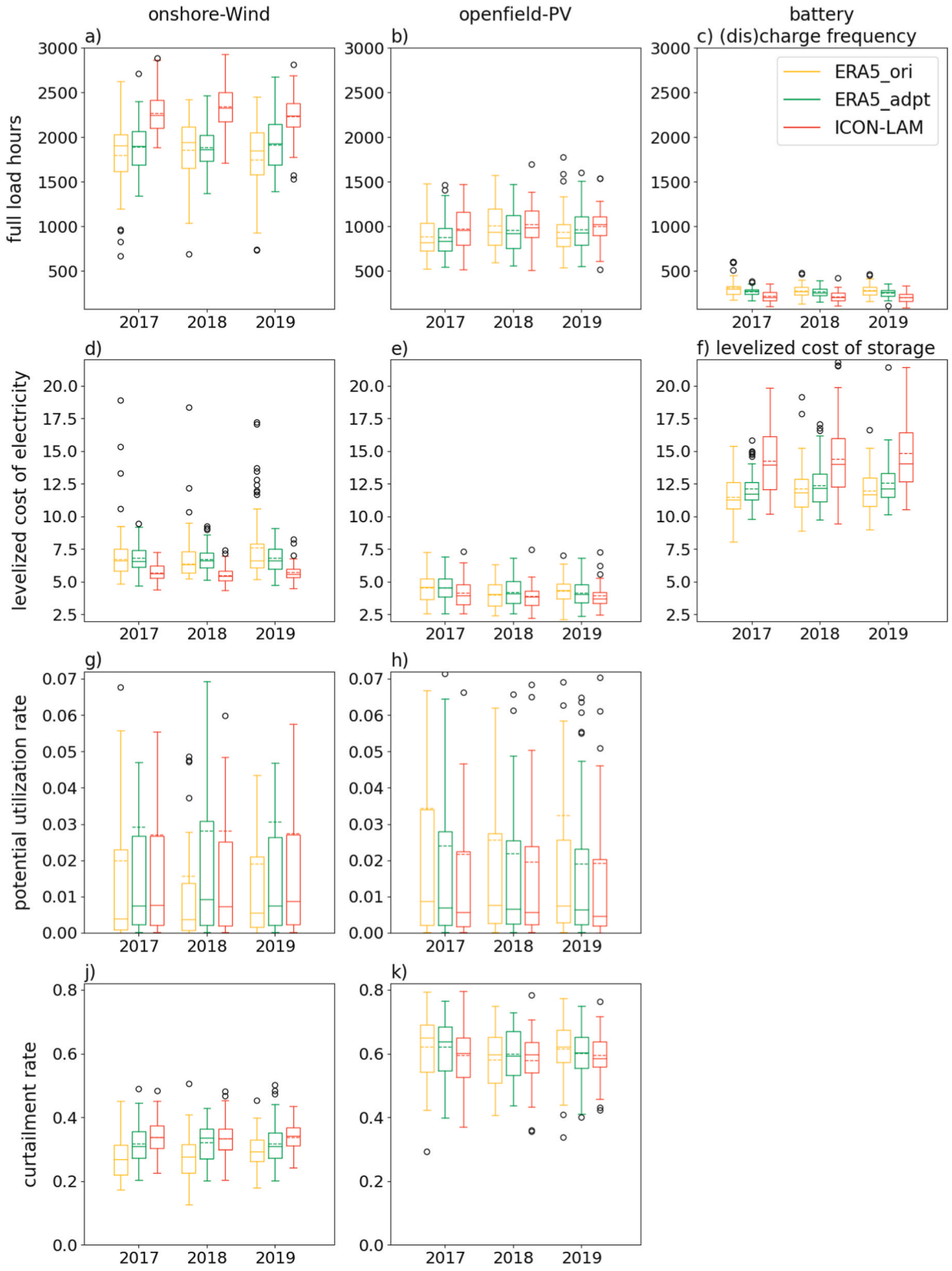

Fig. 5. Annual operational characteristics, including full load hours (FLH, [hours]) (1st row), levelized cost of electricity (LCOE, cents per kilowatt-hour [€/kWh]) (2nd row), potential utilisation rate (3rd row), and curtailment rate (4th row), for onshore wind (1st column), open-field PV (2nd column), and battery (3rd column) technologies used in cost-optimised energy systems designed from different meteorological datasets. Please note that terminology changes when it comes to battery technology. The (dis)charge frequency is the total energy delivered by the battery divided by its capacity, and the levelized cost of storage is the total annual cost of the battery divided by the total energy delivered by the battery. A blank subplot indicates that the corresponding metric does not apply to that particular technology. For the description of the components of boxplots, please refer to Fig. 4.

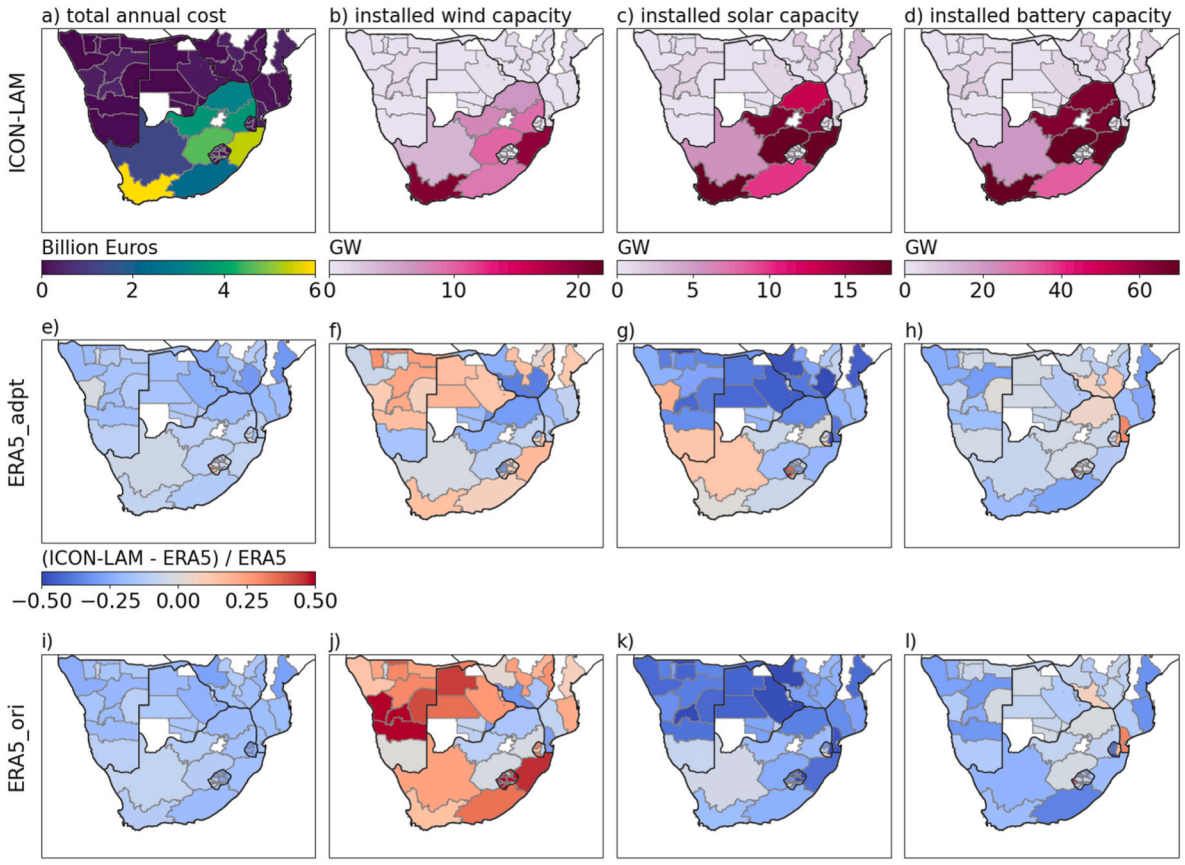

Fig. 6. The costs and design of cost-optimised energy systems in southern Africa derived from meteorological data sets of ICON-LAM (1st row), ERA5_adpt (2nd row), and ERA5_ori (3rd row) based on 2017. For the other years, the reader is directed to Figs. S4 and S5. Energy systems optimised with ERA5 data sets are depicted as relative differences compared to results obtained from ICON-LAM. The regions coloured in white indicate that a cost-optimised energy system incorporating wind, solar, and battery technologies is not feasible in that region without connections to neighbouring regions.

meteorological data sets behave over time is investigated. This is achieved by examining the time series of cost-optimised energy systems, focusing on the shares of electricity demand met by wind energy, solar energy, and batteries. Although the time series is simulated on an hourly basis, as shown in Fig. 7, daily data is analysed to present more condensed information, which nevertheless delivers consistent results, as demand is fully met each hour.

The projected 2050 yearly cycle of daily total electricity demand for the southern African provinces is shown in Fig. 8 and Fig. 9 compares daily electricity demand shares met by wind energy, solar energy, and batteries in energy systems. ICON-LAM generally shows higher shares of wind energy and lower shares of solar energy: 6 % and 18 % for wind and −7 % and −19 % for solar, averaged over all days and all provinces respectively from columns "ICON-LAM minus ERA5_adpt" and "ICON-LAM minus ERA5_ori". Exceptions are found in Lesotho, compared to ICON-LAM, ERA5_adpt uses more (3 %, on average among provinces) wind energy (Fig. 9b LSO) and less (3 %) solar energy (Fig. 9e LSO), while ERA5_ori has an extremely lower (39 %) wind share with a correspondingly higher (41 %) solar share (Fig. 9c and f LSO). This result is consistent with the findings of Chen et al. [34], who show that ICON-LAM has the highest skill of simulating wind speeds over complex terrain, such as over Lesotho, where ERA5_GWA tends to overestimate, especially over extremely contrasting terrain features such as hilltops and ridges. In contrast, ERA5_ori cannot resolve this type of terrain and tends to underestimate due to its coarse spatial resolution.

Wind and solar energy shares, in meeting the electricity demand, vary throughout the year but complement each other, as the system is designed to fully meet electricity demand (see Figs. 1, 2 and 8) at minimal cost. Slightly different temporal patterns of met electricity shares are observed between the years 2017–2019 (see Fig. S6 for 2018 results and Fig. S7 for 2019). The contribution of wind and solar energy to meet the electricity demand on a specific day may vary between years, as it is influenced by the local weather on that day, or even over multiple days, depending on the weather pattern. This interannual variability is therefore expected, but no significant year-to-year changes are noted in the comparison columns of Figs. 9, S6, and S7, indicating consistent results.

In all the cost-optimised energy systems, the total generated power from wind and solar energy most of the time meets the local electricity demand with only a small contribution of battery power. The spatio-temporal average battery discharge rates – the fraction of time when the battery is discharging – are 27.7 %, 32.6 %, and 36.5 % for the cost-optimised energy systems derived from ERA5_ori, ERA5_adpt, and ICON-LAM, respectively, while the corresponding total electricity demand met by the battery is only 6.4 %, 5.3 %, and 5.8 %.

4. Conclusions

Our results indicate that the cost-optimised energy systems in southern Africa, designed based on ICON-LAM meteorological input data, reduces the estimated total annual cost on average by about 14 % (16 % less than ERA5_adpt and 11 % less than ERA5_ori) compared to the commonly used data set for this task, the ERA5 products, and cuts the required battery capacity by 13 % (9 % less than ERA5_adpt and 17 % less than ERA5_ori). In detail, cost-optimised energy systems derived from ICON-LAM, compared to other alternatives, deploy more wind energy (comparable to ERA5_adpt and 9 % more than ERA5_ori), less solar energy (13 % less than ERA5_adpt and 23 % less than ERA5_ori),

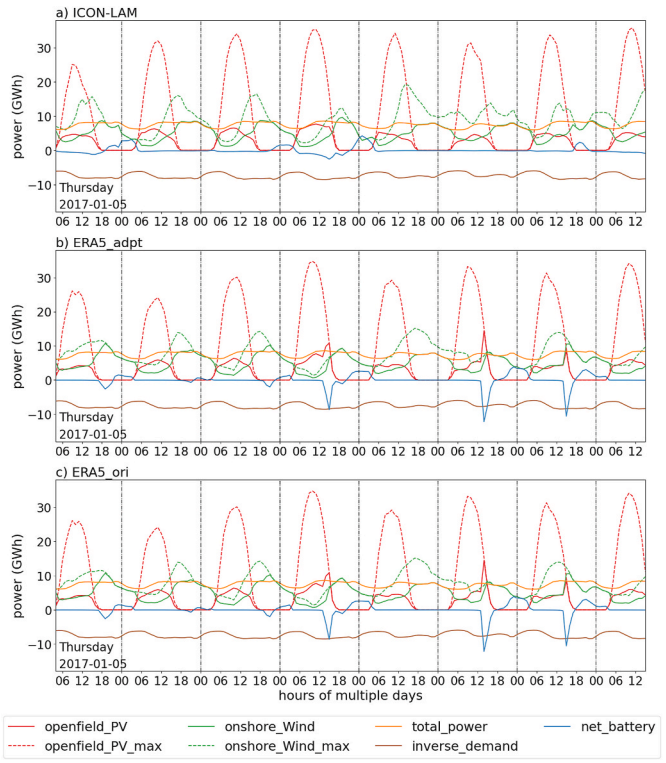

Fig. 7. The time series subset of the cost-optimised energy system of the province Western Cape derived from three different meteorological data sets based on the 2017 weather year. The orange solid line represents the total power generation in the energy system, which is made up of contributions from openfield PV (solar energy) in the red solid line, onshore wind energy in the green solid line, and batteries in the blue solid line. The electricity demand, or energy sink, is presented in the brown solid line. The maximum harvestable solar and wind energy generation is shown in the red and green dashed lines, respectively.

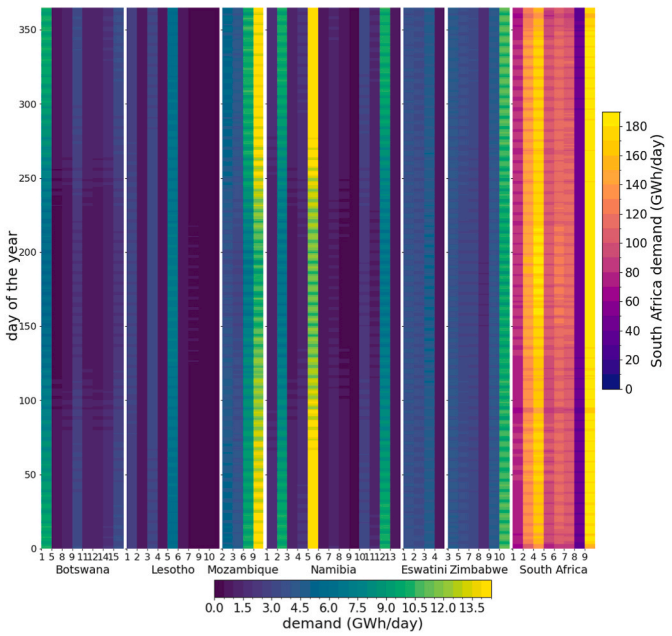

Fig. 8. The projected 2050 daily total electricity demand of the southern African provinces (numbers), where a feasible cost-optimised energy system can be built. The colour bar on the right of the figure, with a different scale, is used exclusively for the electricity demand of South African provinces. This is necessary due to the large difference in electricity demand between provinces in South Africa and other Southern African countries considered in this study. All provinces are arranged by country and sorted ascending by name index, i.e., their identical GID numbers, which are shown in the ticks on the x-axis. For the correspondence between the identical GID numbers and the exact province, please refer to Table S1, column "Province code (GID_1 code)".

and less battery (9 % less than ERA5_adpt and 17 % less than ERA5_ori), primarily due to the cheaper wind energy revealed by ICON-LAM. Under such circumstances, this would facilitate the development of regional renewable net-zero energy systems. This finding further underlines the necessity of using high-resolution, physically consistent model-based data to plan for a cost-optimised energy system. Data sets with longer high-resolution time series and ensemble configurations for uncertainty evaluation, although rare, could provide a valuable complement to the current pilot study.

Our results also show significant differences in wind energy potentials, with ICON-LAM producing, on average, about 5 GWh per turbine (approximately 50 %) more annual wind power compared to other ERA5 products. The additional wind energy per year revealed by ICON-LAM for only one single wind turbine, averaged out of the 1.8 million eligible turbines across the study area, could power approximately 1736 typical British three-person households, the size of a small town, with an annual electricity consumption of 2880 kWh/household [58], for one year. In contrast, the solar energy potentials are similar (almost identical) across all data sets. This suggests that solar irradiance under clear-sky conditions over southern Africa primarily controlled by large-scale anticyclonic atmospheric circulation patterns are well-resolved in all the data sets. The simulation of wind speed remains challenging, particularly for the coarser spatial resolution of ERA5. Local surface properties cannot be resolved in such detail as with the kilometre-scale ICON-LAM, the simulation of planetary boundary layer mixing or surface friction, and ultimately, the accuracy of near-surface wind speed simulations is affected.

Regarding the role of batteries in renewable energy systems, the three meteorological data sets of the study agree with each other that wind and solar can supply most of the electricity demand, with minimal battery use – averaged only about 5.8 % of the annual demand has to be covered by batteries, for about 68 % of the time, no battery discharge is required. Batteries remain essential, however, for times without sufficient wind and solar power. This is in accordance with the global 100 % renewable or net-zero emission scenarios, where batteries are projected to be a critical energy system component to achieving high levels of reliability, although their contribution to electricity demand may vary depending on local conditions and specific system designs [59].

The complementarity of wind and solar energy that we study here is actually a frequently raised topic in the literature. However, many of these studies, especially from the geoscience realm, tend to address the complementarity of wind and solar energy from a theoretical and strategic perspective, and do not consider the latest developments in the field of renewable energy assessment. Compared to our study, these studies do not consider the suitability of the land to build wind turbines or solar power plants or the specific placement of the renewable energy sources, and only include spatially distributed (gridded) meteorological information. Also in these studies, the energy system, which includes the complementarity of wind and solar energy, often does not consider the system costs and the battery capacity, or only includes a predefined constant battery capacity. However, these are important factors that need to be carefully considered in the design and operation of real-world energy systems.

In previous studies within the energy realm that examine the complementarity of wind and solar resources, the latest findings from renewable energy assessments are typically incorporated. However, these studies often rely directly on the available meteorological datasets for their regions of interest. Such data sets, usually coarse-resolution global reanalysis products, lack the spatial detail required for accurate wind energy characterisation. This limitation is particularly pronounced

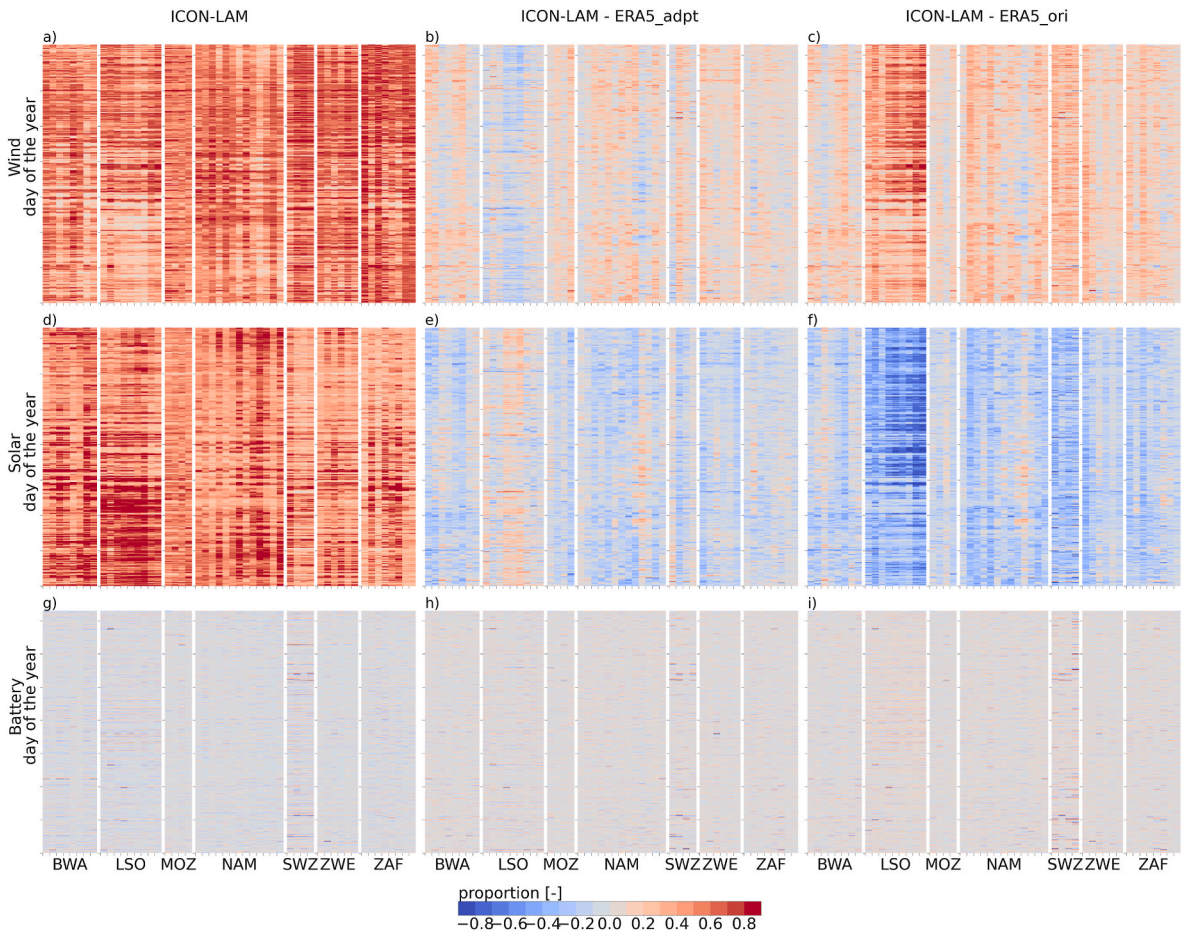

Fig. 9. The time series comparison of daily demand (with reference to the 2050 demand projection) fraction met by wind, solar, and battery technologies in the cost-optimised energy systems derived from meteorological data sets ICON-LAM, ERA5_adpt, and ERA5_ori for 2017. The 1st column is the result derived from ICON-LAM, and the 2nd and 3rd columns are the comparison of ICON-LAM to the ERA5 variants, ICON-LAM minus ERA5_adpt and ICON-LAM minus ERA5_ori, respectively. The structure of the x- and y-axis of each subplot in this figure is the same as in Fig. 8, i.e., the y-axis contains the day of the year and the x-axis shows different provinces grouped by country; the country names are abbreviated (Table S1) for better visualisation. In the "ICON-LAM" column, only positive or 0 values are present in the "Wind" and "Solar" rows, meaning the corresponding fraction of electricity demand is met; both positive and negative values are present in the "Battery" row, indicating battery discharge and charge, respectively. In the columns "ICON-LAM - ERA5_adpt" and "ICON-LAM - ERA5_ori", positive and negative values represent the comparison between ICON-LAM and ERA5 for each technology. The results for the years 2018 and 2019 are shown in Figs. S6 and S7.

in Africa, where data scarcity remains a persistent challenge. In contrast, the present study integrates advancements from both geoscience and energy research, providing insights that have not been explored elsewhere.

It should be noted, however, that the impact of different meteorological data sets on the cost-optimised design of energy systems is specific to our study area in southern Africa, which is the limitation of this study. The region's complex land-atmosphere interactions, influenced by diverse terrain with some highly contrasting features and strong ocean-land circulation patterns, play a role in the simulation of VRE variables and may limit the broader applicability of our findings. Nevertheless, this study highlights the critical need for future VRE-based energy system designs to incorporate high-resolution, dedicated modelling rather than relying solely on readily available data products.

As for the energy systems modelling, this study assumes lossless power transmission and no power exchange between provinces to examine the direct impact on the local energy system. While renewable energy complementarity studies, like in Ref. [60] that incorporate power grid dynamics, interregional power flows, and grid congestion analysis offer valuable insights, their application in Africa remains challenging due to unstable power infrastructure and limited data availability. Furthermore, research by Blanco and Faaij [61] suggests that including more energy sectors reduces the need for battery capacity in the energy systems. By modelling energy systems with only wind and solar energy and without interprovincial transmission, this study may overestimate battery needs. Modelling a real-world full energy system with all the energy sectors integrated and power exchanged would likely lower both battery requirements and overall costs, but the relative differences in VRE contributions derived from different meteorological data sets should remain consistent with the findings of this study.

Furthermore, this study considers annual variations in designing the cost-optimised energy system. Multi-decadal simulations that capture interannual VRE variabilities, as shown by Caglayan et al. [62], could yield more robust results and, therefore, deserve attention in future decades-scale applications of the current study.

CRediT authorship contribution statement

Shuying Chen: Writing – review & editing, Writing – original draft, Visualization, Validation, Software, Resources, Methodology, Investigation, Formal analysis, Data curation, Conceptualization. **Klaus Goergen:** Writing – review & editing, Visualization, Validation, Supervision, Project administration, Methodology, Investigation, Funding acquisition, Formal analysis, Data curation, Conceptualization. **Harrie-Jan Hendricks Franssen:** Writing – review & editing, Validation, Supervision, Resources, Project administration, Methodology,

Investigation, Funding acquisition, Formal analysis, Conceptualization. **David Franzmann:** Writing – review & editing, Visualization, Validation, Software, Resources, Methodology, Investigation, Formal analysis, Data curation, Conceptualization. **Christoph Winkler:** Software, Resources, Methodology, Data curation, Conceptualization. **Shitab Ishmam:** Writing – review & editing, Resources, Data curation. **Stefan Poll:** Software, Resources, Data curation. **Jochen Linssen:** Supervision, Project administration, Funding acquisition. **Harry Vereecken:** Writing – review & editing, Supervision, Project administration, Funding acquisition. **Heidi Heinrichs:** Writing – review & editing, Visualization, Validation, Supervision, Resources, Project administration, Methodology, Investigation, Funding acquisition, Formal analysis, Conceptualization.

Code availability

The Renewable Energy Simulation toolkit for Python (RESKit) model code is available via GitHub (https://github.com/FZJ-IEK3-VSA/RESKit). The Framework for Integrated Energy System Assessment (ETHOS.FINE) can be accessed through GitHub (https://github.com/FZJ-IEK3-VSA/FINE?tab=readme-ov-file). The cost-optimisation solver Gurobi is from Gurobi (https://www.gurobi.com).

Declaration of generative AI and AI-assisted technologies in the writing process

During the preparation of this work, the authors used ChatGPT, DeepL-Write, and Grammarly in order to improve language and readability. After using these tools, the authors reviewed and edited the content as needed and take full responsibility for the content of the publication.

Declaration of competing interest

The authors declare that they have no known competing financial interests or personal relationships that could have appeared to influence the work reported in this paper.

Acknowledgments

This work was supported by the Helmholtz Association under the programs “Energy System Design” and “Earth and Environment, topic Bio-Economy” at the Research Centre Jülich in Germany. The “Vernetzungsdoktorand” programme of the Research Centre Jülich partially funded this work. Part of this work was supported by funding from the Deutsche Forschungsgemeinschaft (DFG, German Research Foundation) – DETECT project SFB 1502/1–2022 – project number: 450058266. The authors gratefully acknowledge the Gauss Centre for Supercomputing eV (GCS, www.gauss-centre.eu) for funding this project by providing computing time through the John von Neumann Institute for Computing (NIC) on the GCS Supercomputer JUWELS at **Jülich** Supercomputing Centre (JSC). The Centre for High-Performance Scientific Computing in Terrestrial Systems at Geoverbund ABC/J is highly appreciated. Open Access funding enabled and organised by Projekt DEAL.

Appendix A. Supplementary data

Supplementary data to this article can be found online at https://doi.org/10.1016/j.energy.2025.139565.

Data availability

The ERA5 dataset was downloaded from C3S (https://doi.org/10.24381/cds.adbb2d47). The Global Wind Atlas V3 can be retrieved from (https://globalwindatlas.info), and the Global Solar Atlas V2 (https://globalsolaratlas.info). The ICON-LAM data is stored at (https://doi.org/10.26165/JUELICH-DATA/JYGQ65).

References

[1] International Energy Agency. Africa energy outlook 2022. Available from: https://www.iea.org/reports/africa-energy-outlook-2022/; 2022.
[2] Winkler C, et al. Participatory mapping of local green hydrogen cost-potentials in Sub-Saharan Africa. Int J Hydrogen Energy 2025;112:289–321.
[3] Ishmam S, et al. Mapping local green hydrogen cost-potentials by a multidisciplinary approach. Int J Hydrogen Energy 2024;87:1155–70.
[4] Moran EF, et al. Advancing convergence research: renewable energy solutions for off-grid communities. Proc Natl Acad Sci 2022;119(49):e2207754119.
[5] Nyarko K, Whale J, Urmee T. Drivers and challenges of off-grid renewable energy-based projects in West Africa: a review. Heliyon 2023;9(6):e16710.
[6] Oteng C, et al. Towards a carbon neutral Africa: a review of the linkages between financial inclusion and renewable energy. Soc Sci Humanit Open 2024;10:100923.
[7] López Prol J, Schill W-P. The economics of variable renewable energy and electricity storage. Annual Review of Resource Economics 2021;13:443–67.
[8] Wang J, et al. Inherent spatiotemporal uncertainty of renewable power in China. Nat Commun 2023;14(1):5379.
[9] Mancarella P. MES (multi-energy systems): an overview of concepts and evaluation models. Energy 2014;65:1–17.
[10] Bale CS, Varga L, Foxon TJ. Energy and complexity: new ways forward. Appl Energy 2015;138:150–9.
[11] Cochran J, et al. Integrating variable renewable energy in electric power markets. Best practices from international experience. Golden, CO (United States): National Renewable Energy Lab.(NREL); 2012.
[12] Sinsel SR, Riemke RL, Hoffmann VH. Challenges and solution technologies for the integration of variable renewable energy sources—a review. Renew Energy 2020;145:2271–85.
[13] Deguenon L, Yamegueu D, Gomna A. Overcoming the challenges of integrating variable renewable energy to the grid: a comprehensive review of electrochemical battery storage systems. J Power Sources 2023;580:233343.
[14] Palys MJ, Daoutidis P. Power-to-X: a review and perspective. Comput Chem Eng 2022;165:107948.
[15] Verdolini E, Vona F, Popp D. Bridging the gap: do fast-reacting fossil technologies facilitate renewable energy diffusion? Energy Policy 2018;116:242–56.
[16] Clack CT, et al. Evaluation of a proposal for reliable low-cost grid power with 100% wind, water, and solar. Proc Natl Acad Sci 2017;114(26):6722–7.
[17] Tong D, et al. Geophysical constraints on the reliability of solar and wind power worldwide. Nat Commun 2021;12(1):6146.
[18] Shaner MR, et al. Geophysical constraints on the reliability of solar and wind power in the United States. Energy Environ Sci 2018;11(4):914–25.
[19] Ren G, et al. Spatial and temporal assessments of complementarity for renewable energy resources in China. Energy 2019;177:262–75.
[20] D'Isidoro M, et al. Estimation of solar and wind energy resources over Lesotho and their complementarity by means of WRF yearly simulation at high resolution. Renew Energy 2020;158:114–29.
[21] Costoya X, et al. Assessing the complementarity of future hybrid wind and solar photovoltaic energy resources for North America. Renew Sustain Energy Rev 2023;173.
[22] Richardson D, Pitman A, Ridder N. Climate influence on compound solar and wind droughts in Australia. npj Clim Atmos Sci 2023;6(1):184.
[23] Jurasz J, et al. A review on the complementarity of renewable energy sources: concept, metrics, application and future research directions. Sol Energy 2020;195:703–24.
[24] Dunnett S, et al. Predicted wind and solar energy expansion has minimal overlap with multiple conservation priorities across global regions. Proc Natl Acad Sci 2022;119(6):e2104764119.
[25] McKenna R, et al. High-resolution large-scale onshore wind energy assessments: a review of potential definitions, methodologies and future research needs. Renew Energy 2022;182:659–84.
[26] Morin B, et al. Reducing RES Droughts through the integration of wind and solar PV. Renew Energy 2025:123392.
[27] Rodriguez M, Arcos–Aviles D, Martinez W. Fuzzy logic-based energy management for isolated microgrid using meta-heuristic optimization algorithms. Appl Energy 2023;335:120771.
[28] Behera S, Dev Choudhury NB. Optimal battery management in PV+ WT micro-grid using MSMA on fuzzy-PID controller: a real-time study. Sustainable Energy Research 2024;11(1):41.
[29] Davidson MR, Millstein D. Limitations of reanalysis data for wind power applications. Wind Energy 2022;25(9):1646–53.
[30] Hersbach H, et al. The ERA5 global reanalysis. Q J R Meteorol Soc 2020;146(730):1999–2049.
[31] GWA. Data obtained from the “Global Wind Atlas 3.0,” a free, web-based application developed, owned and operated by the Technical university of Denmark (DTU). The global wind atlas 3.0 is released in partnership with the world bank group, utilizing data provided by vortex, using funding provided by the energy sector management assistance program (ESMAP). Available from: https://globalwindatlas.info; 2019.
[32] GSA. Data obtained from the “Global Solar Atlas 2.0,” a free, web-based application is developed and operated by the company solargis s.r.o. on behalf of the world bank group, utilizing solargis data, with funding provided by the energy sector management assistance program (ESMAP). Available from: https://globalsolaratlas.info; 2019.

[33] Chen S, et al. Convection-permitting ICON-LAM simulations for renewable energy potential estimates over Southern Africa. J Geophys Res Atmos 2024;129(6).
[34] Chen S, et al. Higher onshore wind energy potentials revealed by kilometer-scale atmospheric modeling. Geophys Res Lett 2024;51(19).
[35] Martínez-Gordón R, et al. A review of the role of spatial resolution in energy systems modelling: lessons learned and applicability to the north sea region. Renew Sustain Energy Rev 2021;141:110857.
[36] Ruiz SAG, Barriga JEC, Martínez JA. Wind power assessment in the Caribbean region of Colombia, using ten-minute wind observations and ERA5 data. Renew Energy 2021;172:158–76.
[37] European Centre for Medium-Range Weather Forecasts (ECMWF). *New climate reanalysis: ERA6*. 2024. Available from: https://www.ecmwf.int/en/about/media-centre/news/2024/copernicus-climate-change-service-provides-new-tools-users.
[38] Gruber K, et al. Towards global validation of wind power simulations: a multi-country assessment of wind power simulation from MERRA-2 and ERA-5 reanalyses bias-corrected with the global wind atlas. Energy 2022;238:121520.
[39] Ryberg DS, et al. The future of European onshore wind energy potential: detailed distribution and simulation of advanced turbine designs. Energy 2019;182:1222–38.
[40] Stratton RA, et al. A Pan-African convection-permitting regional climate simulation with the met office unified model: Cp4-africa. J Clim 2018;31(9):3485–508.
[41] Kendon EJ, et al. Enhanced future changes in wet and dry extremes over Africa at convection-permitting scale. Nat Commun 2019;10(1):1794.
[42] Zängl G, et al. The ICON (ICOsahedral Non-hydrostatic) modelling framework of DWD and MPI-M: description of the non-hydrostatic dynamical core. Q J R Meteorol Soc 2015;141(687):563–79.
[43] GitHub repository. RESKit—Renewable energy simulation toolkit for python. Available from: https://github.com/FZJ-IEK3-VSA/RESKit; 2019.
[44] Peña-Sánchez EU, et al. Towards high resolution, validated and open global wind power assessments. Nature Communications 2025 (accepted).
[45] Ryberg DS. Generation lulls from the future potential of wind and solar energy in eutope. RWTH Aachen University: Energie & Umwelt/Energy & Environment; 2020.
[46] Wiser R, et al. Expert elicitation survey predicts 37% to 49% declines in wind energy costs by 2050. Nat Energy 2021;6(5):555–65.
[47] Ishmam S. Regional Cooperation in Renewable Energy Systems: Insights from Sub-Saharan Africa. 2025 (submitted), Dissertation, RWTH Aachen University.
[48] Richters O, et al. NGFS climate scenarios data set version 3.0. Zenodo; 2022.
[49] Richters O, et al. NGFS climate scenarios database: technical documentation V3. 1. 2022.
[50] Toktarova A, et al. Long term load projection in high resolution for all countries globally. Int J Electr Power Energy Syst 2019;111:160–81.
[51] Franzmann D, et al. Green hydrogen cost-potentials for global trade. Int J Hydrogen Energy 2023;48(85):33062–76.
[52] ETHOS.FINE - Framework for Integrated Energy System Assessment. GitHub repository. Available from:. 2018. https://github.com/FZJ-IEK3-VSA/FINE?tab=readme-ov-file.
[53] Klütz T, et al. Ethos. FINE: a framework for integrated energy system assessment. J Open Source Softw 2025;10(105):6274.
[54] Gurobi Optimizer L. Gurobi optimizer reference manual. 2018.
[55] Schöb T, et al. The role of hydrogen for a greenhouse gas-neutral Germany by 2045. Int J Hydrogen Energy 2023;48(99):39124–37.
[56] Schöb TF. Model-based analysis of greenhouse gas neutral transformation strategies for Germany. Dissertation: RWTH Aachen University; 2024.
[57] Bolson N, Prieto P, Patzek T. Capacity factors for electrical power generation from renewable and nonrenewable sources. Proc Natl Acad Sci 2022;119(52):e2205429119.
[58] IRSAP. How much energy does an average household use?. Available from: https://www.irsap.com/en/blog/average-energy-consumption.
[59] International Renewable Energy Agency. 100% renewable energy scenarios: supporting ambitious policy targets. Available from, https://www.irena.org/Publications/2024/Mar/100pc-renewable-energy-scenarios-Supporting-ambitious-policy-targets; 2024.
[60] Zhang D, et al. Spatially resolved land and grid model of carbon neutrality in China. Proc Natl Acad Sci 2024;121(10):e2306517121.
[61] Blanco H, Faaij A. A review at the role of storage in energy systems with a focus on power to gas and long-term storage. Renew Sustain Energy Rev 2018;81:1049–86.
[62] Caglayan DG, et al. Impact of different weather years on the design of hydrogen supply pathways for transport needs. Int J Hydrogen Energy 2019;44(47):25442–56.